

# CHEMISTRY

---

## AN ASIAN JOURNAL

www.chemasianj.org

### Accepted Article

**Title:** Development of a Pre-assembled TBET Fluorescent Probe for Ratiometric Sensing of Anticancer Platinum(II) Complexes

**Authors:** Jun Xiang Ong and Wee Han Ang

This manuscript has been accepted after peer review and appears as an Accepted Article online prior to editing, proofing, and formal publication of the final Version of Record (VoR). This work is currently citable by using the Digital Object Identifier (DOI) given below. The VoR will be published online in Early View as soon as possible and may be different to this Accepted Article as a result of editing. Readers should obtain the VoR from the journal website shown below when it is published to ensure accuracy of information. The authors are responsible for the content of this Accepted Article.

**To be cited as:** *Chem. Asian J.* 10.1002/asia.202000157

**Link to VoR:** <http://dx.doi.org/10.1002/asia.202000157>

A Journal of



A sister journal of *Angewandte Chemie*  
and *Chemistry – A European Journal*

---

WILEY-VCH

# Development of a Pre-assembled TBET Fluorescent Probe for Ratiometric Sensing of Anticancer Platinum(II) Complexes

Jun Xiang Ong,<sup>[a]</sup> and Wee Han Ang\*<sup>[a, b]</sup>

[a] Dr. J. X. Ong, Prof. W. H. Ang  
Department of Chemistry  
National University of Singapore  
3 Science Drive 3, Singapore 117543 (Singapore)  
E-mail: ang.weehan@nus.edu.sg

[b] Prof. W. H. Ang  
NUS Graduate School for Integrative Sciences and Engineering  
National University of Singapore  
28 Medical Drive, Singapore 117456 (Singapore)

Supporting information for this article is given via a link at the end of the document. ((Please delete this text if not appropriate))

**Abstract:** Fluorescence microscopy has emerged as an attractive technique to probe the intracellular processing of Pt-based anticancer compounds. Herein, we reported the first Through-Bond Energy Transfer (TBET) fluorescent probe **NPR1** designed for sensitive detection and quantitation of Pt<sup>II</sup> complexes. The novel TBET probe was successfully applied for ratiometric fluorescence imaging of anticancer Pt<sup>II</sup> complexes such as cisplatin and JM118 in cells. Capitalizing on the ability of the probe to discriminate between Pt<sup>II</sup> complexes and their Pt<sup>IV</sup> derivatives, the probe was further applied to study the activation of Pt<sup>IV</sup> prodrug complexes that are known to release active Pt<sup>II</sup> species after intracellular reduction.

## Introduction

Cisplatin, carboplatin and oxaliplatin constitute an important class of Pt<sup>II</sup> drugs that are amongst the most widely used and effective cytotoxic agents for cancer therapy (Figure 1).<sup>[1]</sup> However, their efficacies are limited by their high intrinsic toxicities, debilitating side-effects and occurrences of drug resistance.<sup>[2]</sup> To circumvent these limitations, stable octahedral Pt<sup>IV</sup> prodrug scaffolds, derived from therapeutic square-planar Pt<sup>II</sup> complexes but with additional axial ligands, are being developed. These Pt<sup>IV</sup> prodrug complexes are activated via intracellular reduction to release labile Pt<sup>II</sup> species capable of exerting their cytotoxic effects. Pt<sup>IV</sup> prodrug complexes have been proven to be more efficacious than their Pt<sup>II</sup> progenies while causing less toxicities by virtue of their increased aqueous stabilities.<sup>[3]</sup> As a result, a significant body of work has been carried out to create Pt<sup>IV</sup> complexes with highly tuned properties,<sup>[4]</sup> capable of targeting specific cancer cells<sup>[5]</sup> as well as possessing novel modes of actions.<sup>[6]</sup> Several notable Pt<sup>IV</sup> prodrugs that have undergone clinical trials include ormaplatin, iproplatin and satraplatin (Figure 1).

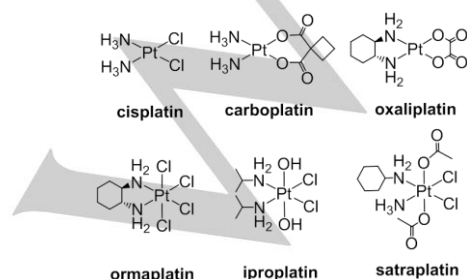


**Figure 1.** FDA-approved Pt<sup>II</sup> drugs and Pt<sup>IV</sup> prodrugs which was clinically evaluated.

There is currently a lack of tools capable of visualizing the uptake and accumulation of Pt-based anticancer compounds directly in cancer cells that would allow researchers to investigate how these compounds are processed at the cellular level. Elemental techniques such as graphite furnace atomic absorption spectrometry (GF-AAS) and inductively-coupled plasma mass spectrometry (ICP-MS) have been applied to quantify Pt content and map cellular localization, but they cannot be applied to live-cell imaging owing to their destructive nature.<sup>[7]</sup> Fluorescence microscopy has emerged as the most effective and employable tool for probing Pt species at the cellular level. The general approach has been to conjugate fluorophores to Pt complexes to track their movement using fluorescence imaging. Using this strategy, Pt<sup>II</sup> drugs such as cisplatin and carboplatin have been conjugated with various fluorophores to probe their intracellular processing *in vitro*.<sup>[8]</sup> Fluorescent ligands have been also attached to axial positions of Pt<sup>IV</sup> prodrug complexes to monitor the reduction process.<sup>[9]</sup> However, modification of Pt<sup>II</sup>/Pt<sup>IV</sup> complexes with such bulky organic groups can significantly alter their drug uptake characteristics and pharmacokinetics, rendering them different from the parent drugs.<sup>[10]</sup>

We and others have been developing exogenous Pt-selective fluorescent probes and applying them intracellularly to study the cellular processing of Pt anticancer compounds. Unlike conjugated fluorophores, these probes are delinked from their intended Pt analyte but selectively bind Pt to trigger a fluorogenic response. New and co-workers reported a fluorescein-based probe linked to a dithiocarbamic acid moiety and a rhodamine-based probe incorporating phenyl isothiocyanate to study the metabolism of Pt<sup>II</sup> drugs.<sup>[11]</sup> Our group developed a rhodamine-based fluorescent turn-on probe as well as a FRET-based ratiometric derivative utilising dithiocarbamates as recognition motifs to study the intracellular activation of Pt<sup>IV</sup> carboxylate prodrug complexes in cells.<sup>[12]</sup> To date, these aforementioned small-molecule probes are the only reported fluorescent probes applied intracellularly to study Pt anticancer compounds. This research space is still largely unexplored and there is a need to expand the library of these probes to improve their scope and detection efficiencies.

Recently, there has been a growing interest in ratiometric fluorescent probes based on Through-Bond Energy Transfer (TBET). In a TBET system, donor and acceptor fluorophores are linked via electronically conjugated spacers and energy transfer occurs through the conjugated bond without the need for spectral overlap.<sup>[13]</sup> This unique feature endows TBET fluorescent probes with high energy transfer efficiencies and large pseudo-Stokes shifts. The TBET mechanism has been utilized in the design of rhodamine-based fluorescent probes for ratiometric sensing of various analytes. In particular, such chemosensors can be derived from pre-assembled ratiometric

TBET scaffolds and subsequently derivatized to detect specific analytes.<sup>[14]</sup> These TBET precursors serve as versatile platforms whereby the 2'-carboxy position could readily condense with amino-containing receptors to generate ratiometric sensors of various analytes based on the TBET mechanism. Inspired by this strategy, we fabricated a novel TBET ratiometric dyad from a naphthalimide-rhodamine platform for selective sensing of Pt<sup>II</sup>. The TBET dyad was subsequently applied for the ratiometric fluorescence imaging of Pt<sup>II</sup> drugs as well as to study the activation of Pt<sup>IV</sup> prodrug complexes in cells. To the best of our knowledge, this is the first report of a TBET-based ratiometric sensor for Pt-based anticancer complexes.

## Results and Discussion

### Probe Design

The ratiometric TBET dyad comprised a naphthalimide donor fluorophore tethered to a rhodamine acceptor fluorophore via a rigid phenylacetylene linker as shown in Figure 2. Diethyldithiocarbamate (DDTC) was chosen as the recognition motif which would be attached at the 2'-position of the TBET platform for the detection of Pt<sup>II</sup> complexes such as cisplatin. This design was based on the reported Rho-DDTC scaffold which elicited a fluorescence turn-on response upon Pt<sup>II</sup> binding.<sup>[12a, 12b]</sup> In order to engineer a ratiometric response, a naphthalimide donor moiety was installed on Rho-DDTC to serve as the donor fluorophore for excitation. The rigid phenylacetylene linker was essential to allow electronic coupling between the naphthalimide donor and rhodamine acceptor fluorophores but at the same time, prevented them from adopting coplanarity and behaving as an extended conjugated system. Therefore upon excitation of the naphthalimide donor, energy would be transferred "through-bond" via the phenylacetylene linker to the rhodamine B acceptor fluorophore.

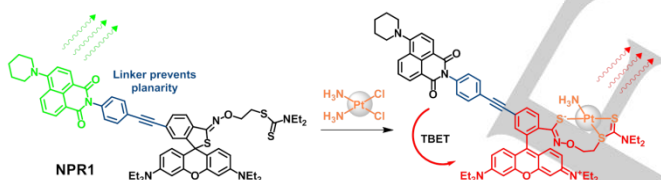


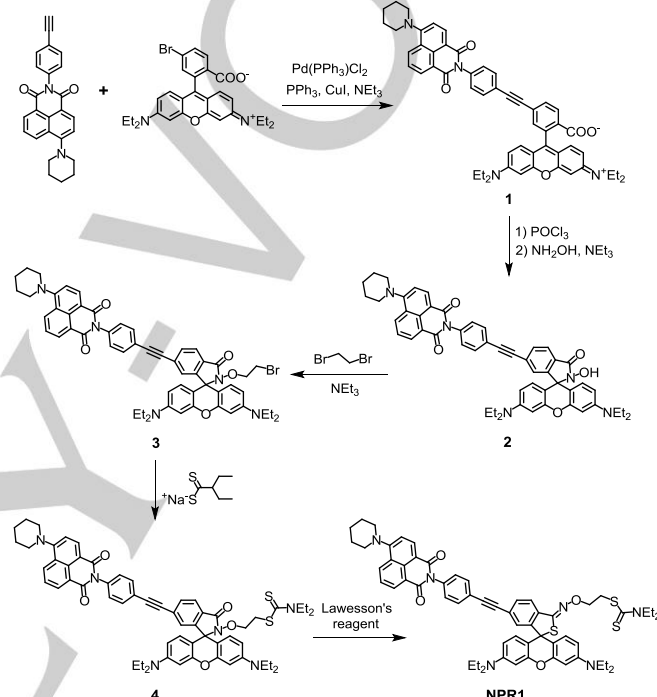
**Figure 2.** Proposed TBET probe for ratiometric sensing of cisplatin.

In keeping with our previous findings, we postulated that the activation of **NPR1** would take place through a two-step mechanism culminating in spiro-ring opening.<sup>[12]</sup> The initial binding of DDTC to cisplatin and its structural analogues would result in the displacement of one of the ammine or chloride ligands. The thiocarbonyl group on the DDTC recognition motif would labilise the *trans*-ligand on Pt via *trans*-effect, promoting reaction with the spirothiophene motif and triggering spiro-ring opening. This would allow energy to be transferred from the donor to the rhodamine B acceptor when **NPR1** is excited, resulting in emission from rhodamine B fluorophore (red emission). In the absence of spiro-ring opening, however, TBET would not occur and only emission from the donor naphthalimide fluorophore (green emission) would be observed upon **NPR1** excitation. By measuring in parallel these emission intensities from the donor and acceptor fluorophores, Pt<sup>II</sup> species could be ratiometrically quantitated.

### Synthesis and Characterization

The naphthalimide-rhodamine ratiometric TBET probe was synthesized as shown in Scheme 1. The naphthalimide donor was synthesized from 4-iodoaniline (Scheme S1). 4-iodoaniline was first treated with trimethylsilylacetylene under Sonogashira coupling conditions to afford 4-[(trimethylsilyl)ethynyl]aniline. Deprotection of 4-[(trimethylsilyl)ethynyl]aniline with K<sub>2</sub>CO<sub>3</sub> gave

4-ethynylaniline which was subsequently reacted with 4-piperidinyl-naphthalic anhydride in an amide condensation reaction to afford *N*-(phenylacetylene)-4-piperidinyl-naphthalimide in good yield. *N*-(phenylacetylene)-4-piperidinyl-naphthalimide was then subjected to Sonogashira coupling with 5'-Br-rhodamine B to give the naphthalimide-rhodamine TBET scaffold **1**. Treatment of **1** sequentially with POCl<sub>3</sub> and NH<sub>2</sub>OH yielded the hydroxamate derivative, **2**. Reaction of **2** with excess 1,2-dibromoethane in the presence of Et<sub>3</sub>N as the base yielded **3**, which was converted to **4** when treated with NaDDTC. Lastly, **4** was treated with Lawesson's reagent in benzene to furnish the target compound **NPR1** which was fully characterized by <sup>1</sup>H NMR, <sup>13</sup>C{<sup>1</sup>H} NMR and ESI-MS.



**Scheme 1.** Synthetic route to prepare ratiometric TBET dyad **NPR1**.

### Photophysical properties of **NPR1**

The photophysical properties of **NPR1** in CH<sub>3</sub>CN/HEPES buffer (v/v=7:3, 5 mM, pH 7.4) were investigated. In the absence of Pt<sup>2+</sup>, **NPR1** displayed a broad absorption band centered at 418 nm attributed to the naphthalimide moiety. With the addition of K<sub>2</sub>PtCl<sub>4</sub> (0–8 eq.), a new absorption band centered at 565 nm appeared gradually, accompanied by a colour change from yellow to pink, corresponding to the rhodamine acceptor (Figure 3a and Figure S1). Upon excitation of the free **NPR1** at 420 nm, an emission band centered at 545 nm was observed. There was no energy transfer in the free probe as the rhodamine acceptor was in the closed-ring form and therefore only emission from the naphthalimide donor was observed.

Upon addition of K<sub>2</sub>PtCl<sub>4</sub> (0–8 eq.), the intensity of the emission band at 545 nm decreased in intensity and simultaneously a new emission band at 595 nm increased in intensity (Figure 3b). This observation was ascribed to increased TBET from naphthalimide donor to rhodamine acceptor following spiro-ring opening of the spirothiophene induced by Pt<sup>2+</sup>. At the same time, the emission colour of the solution turned from yellowish-green to orange-red (Figure 3a). The ratio of emission intensities of rhodamine to naphthalimide (I<sub>595</sub>/I<sub>545</sub>) varied from 0.7 in the absence of Pt<sup>2+</sup> to 20.9 in the presence of 8 equivalents of Pt<sup>2+</sup>, corresponding to 30-fold enhancement in the ratios. **NPR1** also showed a linear relationship between the emission ratios with increasing concentrations of Pt<sup>2+</sup> suggesting that it was potentially useful for quantitative determination of Pt<sup>2+</sup>. The energy transfer efficiency of **NPR1** was calculated to be as

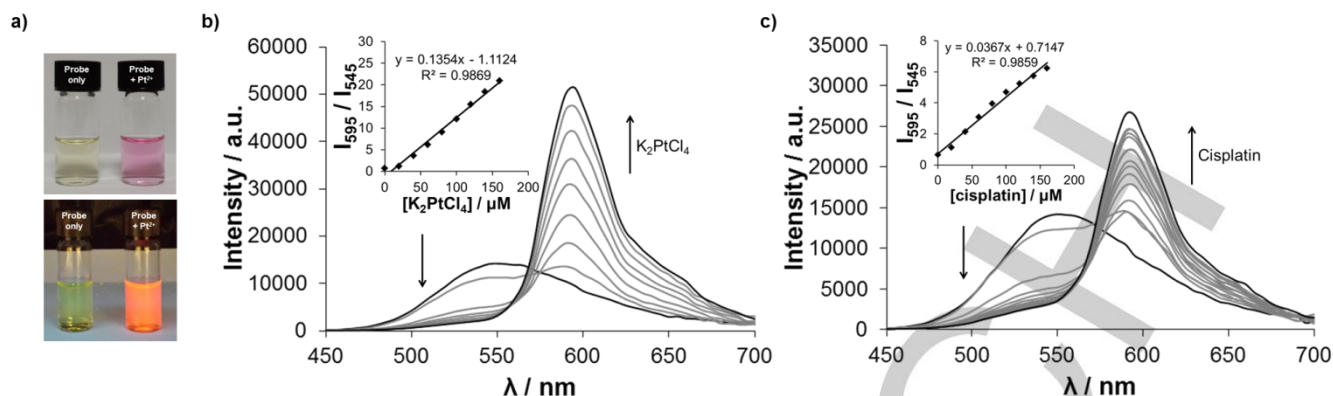


**Figure 3.** (a) Colour change (top) and fluorescence change (bottom) before and after addition of  $K_2PtCl_4$  to **NPR1**. (b) Fluorescence spectra of **NPR1** (20  $\mu$ M) in response to the presence of  $Pt^{2+}$  (0–8 eq.) in  $CH_3CN/HEPES$  buffer ( $v/v=7:3$ , 5 mM, pH 7.4) ( $\lambda_{ex}=420$  nm). Inset: Linear plot of emission ratios ( $I_{595}/I_{545}$ ) against  $Pt^{2+}$  concentrations (0–160  $\mu$ M). (c) Fluorescence spectra of **NPR1** (20  $\mu$ M) in response to cisplatin (0–14 eq.) in  $CH_3CN/HEPES$  buffer ( $v/v=7:3$ , 5 mM, pH 7.4). Inset: Calibration curve showing range (0–160  $\mu$ M) of linear dependence. The slope was used for the calculation of the detection limit of cisplatin.

high as 91 % which is expected of a TBET dyad (Figure S2).<sup>[14b]</sup> Job's plot analysis also revealed that **NPR1** binds to  $Pt^{2+}$  in a 1:1 ratio (Figure S3). Time-dependent fluorescence response studies revealed that the fluorescence intensity ratios increased linearly over time in the presence of  $Pt^{2+}$  and remained constant after 150 min (Figure S4).

#### Selectivity and pH response

Fluorescence measurements of the TBET probe with various metal ions (3 eq.) revealed excellent selectivity for  $Pt^{2+}$ . **NPR1** did not give any observable response in the presence of biologically-relevant metal ions such as  $Na^+$ ,  $K^+$ ,  $Mg^{2+}$ ,  $Cu^{2+}$ ,  $Ni^{2+}$ ,  $Zn^{2+}$ ,  $Fe^{2+}$  and  $Fe^{3+}$  (Figure S5 and Figure S6). In addition, the colour of the solutions remained yellow indicating that the probe was not activated in the presence of other metal ions (Figure S7). **NPR1** was stable over a wide pH range 3–11 as variations in pH did not alter the fluorescence ratio ( $I_{595}/I_{545}$ ) of the free probe, indicating the closed-ring form of the spirothiophene was retained (Figure S8). The activation of the probe in the presence of  $Pt^{2+}$  was pH-dependent. Fluorescence turn-on responses ( $I_{595}/I_{545}$ ) increased as the pH of the solutions decreased, with significant activation of the probe observed in the pH range 3–10. Since intracellular pH typically ranged from 5–8, **NPR1** was expected to function adequately in a cellular environment with negligible background fluorescence.

#### Ratiometric detection of cisplatin

Having ascertained that ratiometric detection of  $Pt^{2+}$  metal ion was feasible, the ability of **NPR1** to perform ratiometric detection of anticancer  $Pt^{II}$  complexes such as cisplatin was investigated. **NPR1** was titrated with cisplatin (0–14 eq.) in  $CH_3CN/HEPES$  buffer ( $v/v=7:3$ , 5 mM, pH 7.4) and fluorescence measurements were recorded. As shown in Figure 3c, titration of **NPR1** with cisplatin resulted in good ratiometric response, in keeping with  $Pt^{2+}$ . A good linear working range was observed from the addition of 0–160  $\mu$ M of cisplatin in the titration experiment signifying its potential for quantitative determination of cisplatin. The detection limit ( $3\sigma/slope$ )<sup>[15]</sup> for cisplatin was determined to be 202 nM which was sufficiently low enough to detect micromolar doses of cisplatin typically administered. The selectivity of the probe towards cisplatin was high and competitive experiments showed that the presence of other metal ions did not interfere with detection of cisplatin (Figure S9). The high sensitivity and selectivity makes **NPR1** a good candidate for the ratiometric sensing of  $Pt^{II}$  anticancer compounds in biological systems.

#### Differentiation of $Pt^{II}$ from $Pt^{IV}$ complexes

Apart from cisplatin, activation of **NPR1** was notable in several other  $Pt^{II}$  anticancer compounds such as JM118, picoplatin,

pyriplatin and carboplatin (Figure 4 and Figure S10). The binding of these  $Pt^{II}$  complexes to the probe induced spiro-ring opening of the spirothiophene leading to TBET turn-on, which allowed for ratiometric sensing of these  $Pt^{II}$  drugs. On the other hand,  $Pt^{IV}$  complexes containing chelating ammine ligands such as oxaliplatin and  $Pt(en)Cl_2$  resulted in no activation of the probe due to the inability of the dithiocarbamate recognition motif to displace the stable ammine chelate.<sup>[12]</sup> As expected, **NPR1** was able to differentiate between  $Pt^{II}$  and  $Pt^{IV}$  metal centers by virtue of their chemical reactivity.  $Pt^{IV}$  complexes such as  $cP-(OH)_2$ ,  $cP-(OBz)_2$ ,  $cP-(OAc)_2$  and satraplatin, derived from cisplatin and JM118 pharmacophores, did not result in activation of the probe. Since  $Pt^{IV}$  prodrug complexes undergo intracellular reduction to release active  $Pt^{II}$  species, **NPR1** would be an ideal tool to study the uptake and activation of  $Pt^{IV}$  prodrugs.

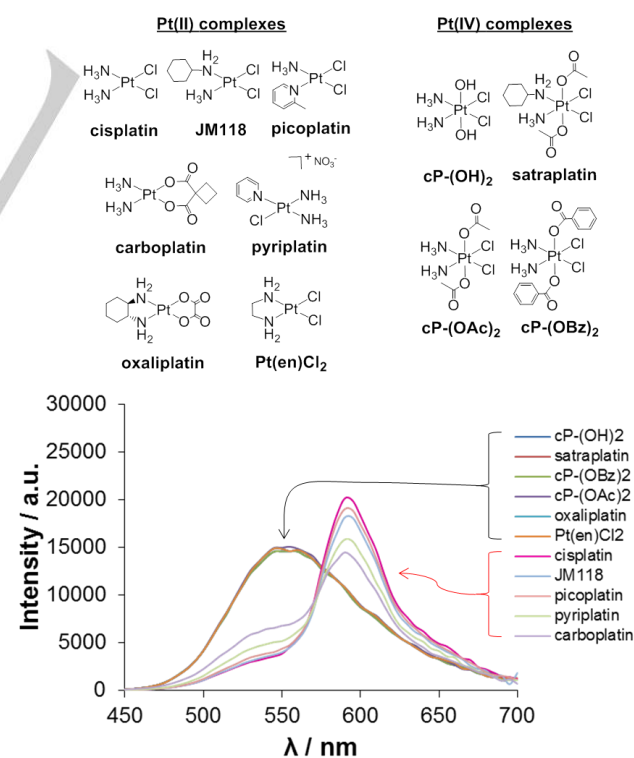


**Figure 4.** (Top) Chemical structures of various  $Pt^{II}$  and  $Pt^{IV}$  complexes. (Bottom) Fluorescence spectra of **NPR1** (20  $\mu$ M) after treatment with various  $Pt^{II}$  and  $Pt^{IV}$  complexes (5 eq.) in  $CH_3CN/HEPES$  buffer ( $v/v=7:3$ , 5 mM, pH 7.4) ( $\lambda_{ex}=420$  nm).

### Fluorescence imaging of NPR1 *in vitro*

**NPR1** was applied for ratiometric fluorescence imaging of Pt-based anticancer complexes in biological systems. HeLa cells were treated with cisplatin (30  $\mu$ M) for 3 h, fixed with 4 % paraformaldehyde, and further incubated with **NPR1** (20  $\mu$ M) for 4 h at 37  $^{\circ}$ C. The cells stained with probe only displayed strong green intracellular fluorescence of naphthalimide and negligible red fluorescence of rhodamine B indicating the cell membrane was permeable to **NPR1**. The incubation of cisplatin-treated cells with the probe exhibited significant increase in red fluorescence accompanied by partial decrease in green fluorescence (Figure 5). These results were consistent with the emission profile of **NPR1** in the presence of cisplatin in aqueous solutions. The emission profile indicated that cisplatin was distributed within the cytoplasm. Based on time-course experiments, maximum emission intensities occurred within 3-4 h treatment after which free cisplatin taken up was bound to other biomolecules. Similar trend was observed when the cells were treated with JM118 (30  $\mu$ M) (Figure S11).

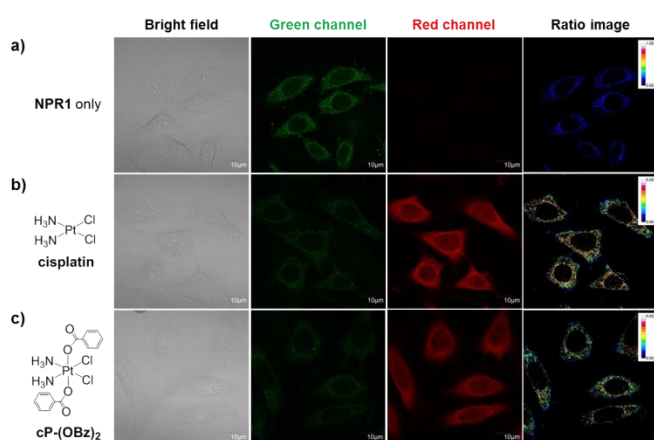


**Figure 5.** Fluorescence images of HeLa cells treated with cisplatin and Pt<sup>IV</sup> complex (30  $\mu$ M). a) Untreated (probe only), and exposed to b) cisplatin and c) cP-(OBz)<sub>2</sub> for 3 h, fixed with 4 % paraformaldehyde and further incubation with **NPR1** (20  $\mu$ M) for 4 h at 37  $^{\circ}$ C.

The excellent ratiometric response of **NPR1** in the presence of cisplatin and JM118 in cells prompted us to investigate the ability of **NPR1** to monitor the intracellular activation of Pt<sup>IV</sup> prodrug complexes in biological systems, specifically those that are based on the cisplatin and JM118 templates. HeLa cells were treated with cP-(OBz)<sub>2</sub> (30  $\mu$ M), which contained the cisplatin drug motif, for 3 h and further incubated with **NPR1** (20  $\mu$ M) for 4 h at 37  $^{\circ}$ C. As shown in Figure 5, cP-(OBz)<sub>2</sub>-treated cells displayed fluorescence turn-on in the red channel indicating the fast conversion of cP-(OBz)<sub>2</sub> to the active Pt<sup>II</sup> species. A similar trend was observed for satraplatin (30  $\mu$ M), which underwent intracellular reduction to release JM118 (Figure S11). Taken together, the results showed that **NPR1** can be applied to monitor the intracellular reduction of Pt<sup>IV</sup> prodrug complexes to further our understanding on how this new class of Pt<sup>IV</sup> prodrugs were being processed intracellularly.

### Conclusion

In summary, a novel TBET fluorescent probe **NPR1** based on the naphthalimide-rhodamine dyad conjugated to a dithiocarbamate recognition motif was successfully synthesized for sensing of Pt-based anticancer compounds. Excellent ratiometric fluorescence turn-on responses were exhibited for a panel of Pt<sup>II</sup> anticancer drugs. The probe also possessed high selectivity and was stable over a wide pH range making it compatible with physiological conditions. *In vitro* studies showed

that **NPR1** was cell-permeable and could be applied for ratiometric fluorescence imaging of anticancer Pt<sup>II</sup> complexes such as cisplatin. Capitalizing on the ability of **NPR1** to differentiate between Pt<sup>IV</sup> prodrug complexes and their reduced Pt<sup>II</sup> products, we successfully applied the probe to monitor the intracellular activation of several Pt<sup>IV</sup> complexes *in vitro*. We believed that this novel TBET probe will serve as an excellent tool for researchers to acquire a better understanding of how Pt<sup>II</sup>/Pt<sup>IV</sup> complexes are processed at the cellular level.

### Experimental Section

#### Materials and instrumentation

All reagents were purchased from commercial vendors and used without further purification. 5'-Br-Rhodamine B was synthesized according to literature methods.<sup>[16]</sup> Cisplatin,<sup>[17]</sup> Pt(en)Cl<sub>2</sub>,<sup>[18]</sup> picoplatin,<sup>[19]</sup> pyriplatin,<sup>[20]</sup> cP-(OH)<sub>2</sub>,<sup>[4a]</sup> cP-(OBz)<sub>2</sub><sup>[4a]</sup> and cP-(OAc)<sub>2</sub><sup>[4a]</sup> were prepared in accordance with literature procedures. Satraplatin, JM118, oxaliplatin and carboplatin were purchased from commercial vendors. <sup>1</sup>H NMR and <sup>13</sup>C{<sup>1</sup>H} NMR spectra were recorded on a Bruker Avance 300 MHz and 500 MHz model. Chemical shifts are reported in parts per million relative to residual solvent peaks. Electro-spray ionization mass spectrometry spectra were obtained on a Thermo Finnigan MAT ESI-MS system. UV-vis spectra were recorded on a Shimadzu UV-1800 UV-vis spectrophotometer. Emission fluorescence spectra were recorded on a JOBIN YVON Fluorolog by HORIBA with iHR320 detector. Fluorescence images were captured with Olympus FluoView FV1000 (Olympus, Japan) laser scanning confocal microscope, with 488 nm laser as the excitation source.

#### Synthesis of 4-piperidinylnaphthalic anhydride

4-bromonaphthalic anhydride (300 mg, 1.08 mmol) and piperidine (0.197 mL, 2 mmol) were refluxed in 2-methoxyethanol for 6 h. After the reaction, solvent was removed and the crude residue purified by column chromatography (100 % CH<sub>2</sub>Cl<sub>2</sub>) to give the product as orange solid. Yield: 260 mg (85.8%, R<sub>f</sub> = 0.5). <sup>1</sup>H NMR (300 MHz, CDCl<sub>3</sub>):  $\delta$  8.57 (1H, d), 8.49 (1H, d), 8.44 (1H, d), 7.71 (1H, t), 7.20 (1H, d), 3.30 (4H, t), 1.90 (4H, m), 1.76 (2H, q).

#### Synthesis of 4-[(trimethylsilyl)ethynyl]aniline

4-iodoaniline (1 g, 4.56 mmol), PdCl<sub>2</sub>(PPh<sub>3</sub>)<sub>2</sub> (88 mg, 0.13 mmol) and Cul (22 mg, 0.12 mmol) were added in a round-bottom flask followed by evacuation/flushing with N<sub>2</sub> for three times. Et<sub>3</sub>N (20 mL) was added and stirred for 30 min. Trimethylsilylacetylene (0.78 mL, 5.5 mmol) was subsequently added and the reaction mixture was heated at 70  $^{\circ}$ C for 12 h. Water (20 mL) was added to the reaction mixture and extracted with EtOAc (3x 25 mL). The organic layers were combined, washed with brine (50 mL) and dried over Na<sub>2</sub>SO<sub>4</sub>. The solvent was removed and the crude residue purified by column chromatography (1:3 v/v EtOAc:hexane) to give the product as yellow solid. Yield: 750 mg (87.7%, R<sub>f</sub> = 0.43). <sup>1</sup>H NMR (300 MHz, CDCl<sub>3</sub>):  $\delta$  7.27 (2H, d), 6.58 (2H, d), 3.71 (2H, br), 0.23 (9H, s).

#### Synthesis of 4-ethynylaniline

4-[(trimethylsilyl)ethynyl]aniline (750 mg, 4 mmol) was dissolved in CH<sub>2</sub>Cl<sub>2</sub>/MeOH (1:1) (30 mL), followed by the addition of K<sub>2</sub>CO<sub>3</sub> (2.82 g, 20.4 mmol). The reaction mixture was stirred at r.t. for 12 h. Water (30 mL) was added to quench the reaction and extracted with CH<sub>2</sub>Cl<sub>2</sub> (3x 20 mL). The organic layers were combined, washed with brine (50 mL) and dried over Na<sub>2</sub>SO<sub>4</sub>. The solvent was removed and the crude residue purified by column chromatography (1:3 v/v EtOAc:hexane) to give the product as yellow solid. Yield: 330 mg (70.5%, R<sub>f</sub> = 0.33). <sup>1</sup>H NMR (300 MHz, CDCl<sub>3</sub>):  $\delta$  7.30 (2H, d), 6.59 (2H, d), 3.82 (2H, br), 2.96 (1H, s).

### Synthesis of *N*-(phenylacetylene)-4-piperidinylnaphthalimide

4-ethynylaniline (224.2 mg, 1.91 mmol), 4-piperidinylnaphthalic anhydride (490 mg, 1.74 mmol) and Zn(OAc)<sub>2</sub> (319.4 mg, 1.74 mmol) were refluxed in pyridine (10 mL) for 48 h. After the reaction, the solvent was removed and the crude residue purified by column chromatography (3:1 v/v CH<sub>2</sub>Cl<sub>2</sub>:hexane) to give the product as yellow solid. Yield: 512 mg (77.6%, R<sub>f</sub> = 0.41). <sup>1</sup>H NMR (300 MHz, CDCl<sub>3</sub>): δ 8.61 (1H, d), 8.53 (1H, d), 8.48 (1H, d), 7.72 (1H, m), 7.65 (2H, d), 7.28 (2H, d), 7.23 (1H, d), 3.28 (4H, t), 3.13 (1H, s), 1.93 (4H, m), 1.76 (2H, m).

### Synthesis of 1

5'-Br-Rhodamine B (390.1 mg, 0.75 mmol), *N*-(phenylacetylene)-4-piperidinylnaphthalimide (285.3 mg, 0.75 mmol), PdCl<sub>2</sub>(PPh<sub>3</sub>)<sub>2</sub> (53.9 mg, 0.077 mmol), PPh<sub>3</sub> (40.0 mg, 0.154 mmol) and CuI (7.5 mg, 0.039 mmol) in THF/Et<sub>3</sub>N (4:1) (40 mL) were refluxed for 18 h under N<sub>2</sub>. The solvent was removed and the crude residue purified by column chromatography (95:5 v/v CH<sub>2</sub>Cl<sub>2</sub>:MeOH) to give the product as red solid. Yield: 280 mg (45.5% R<sub>f</sub> = 0.32). <sup>1</sup>H NMR (500 MHz, CDCl<sub>3</sub>): δ 8.58 (1H, d), 8.51 (1H, d), 8.45 (1H, d), 8.05 (1H, d), 7.70-7.75 (2H, m), 7.61 (2H, d), 7.37 (1H, d), 7.28 (2H, d), 7.19 (1H, d), 6.79 (2H, d), 6.48-6.53 (4H, m), 3.43 (8H, q), 3.26 (4H, t), 1.89 (4H, m), 1.74 (2H, m), 1.21 (12H, t). ESI-MS: *m/z* 821.5 [M+H]<sup>+</sup>.

### Synthesis of 2

**1** (280 mg, 0.34 mmol) in 1, 2-dichloroethane (5 mL) was added POCl<sub>3</sub> (0.4 mL) dropwise over 3 min. The reaction mixture was refluxed for 5 h. The solvent was evaporated to give the crude acid chloride as violet-red oil. The crude acid chloride was dissolved in CH<sub>3</sub>CN (5 mL) and added drop-wise to a THF/H<sub>2</sub>O (5:1) (6 mL) mixture containing hydroxylamine hydrochloride (0.380 g, 5.5 mmol) and Et<sub>3</sub>N (1.2 mL, 8.7 mmol). The reaction mixture was stirred at r.t. for 12 h. The reaction mixture was extracted with CH<sub>2</sub>Cl<sub>2</sub> (3x 10 mL). The organic layers were combined and dried over Na<sub>2</sub>SO<sub>4</sub>. The solvent was removed and the crude residue purified by column chromatography (3:1 v/v EtOAc:hexane) to give the product as yellow solid. Yield: 60 mg (21.1% R<sub>f</sub> = 0.50). <sup>1</sup>H NMR (500 MHz, CDCl<sub>3</sub>): δ 8.59 (1H, d), 8.52 (1H, d), 8.44 (1H, d), 7.85 (1H, d), 7.70 (1H, t), 7.59 (2H, d), 7.26-7.58 (3H, m), 7.20 (1H, d), 6.57 (2H, m), 6.45 (2H, s), 6.34 (2H, m), 3.36 (8H, q), 3.26 (4H, t), 1.90 (4H, m), 1.74 (2H, m), 1.19 (12H, t). ESI-MS: *m/z* 836.3 [M+H]<sup>+</sup>.

### Synthesis of 4

**2** (60 mg, 0.072 mmol) was dissolved in DMF (2 mL) to which Et<sub>3</sub>N (0.098 mL, 0.72 mmol) and 1, 2-dibromoethane (0.124 mL, 1.44 mmol) were added. The reaction mixture was then heated at 60 °C for 4 h. The solvent was removed and CH<sub>2</sub>Cl<sub>2</sub> (15 mL) was added to the residue. The organic layer was washed with water (10 mL) and NaHCO<sub>3</sub> (10 mL), and dried over Na<sub>2</sub>SO<sub>4</sub>. The solvent was removed and the crude residue purified by column chromatography (1:2 v/v EtOAc:hexane) to give the intermediate compound **3** as yellow solid. Yield: 32 mg (47.8% R<sub>f</sub> = 0.48). **3** (32 mg, 0.034 mmol) was dissolved in DMF (1 mL) and NaDDTC (16.2 mg, 0.070 mmol) was added. The reaction mixture was then heated at 60 °C for 12 h. The solvent was removed and CH<sub>2</sub>Cl<sub>2</sub> (15 mL) was added to the residue. The organic layer was washed with water (10 mL) and brine (10 mL), and dried over Na<sub>2</sub>SO<sub>4</sub>. The solvent was removed and the crude residue purified by column chromatography (1:2 v/v EtOAc:hexane) to give the product as yellow solid. Yield: 30 mg (88.2%, R<sub>f</sub> = 0.33). <sup>1</sup>H NMR (500 MHz, CDCl<sub>3</sub>): δ 8.59 (1H, d), 8.52 (1H, d), 8.44 (1H, d), 7.92 (1H, d), 7.70 (1H, t), 7.65 (1H, m), 7.59 (2H, d), 7.26-7.28 (3H, m), 7.20 (1H, d), 6.59 (2H, m), 6.35-6.40 (4H, m), 3.98 (4H, m), 3.73 (2H, q), 3.35-3.42 (10H, m), 3.26 (4H, t), 1.90 (4H, m), 1.74 (2H, m), 1.19-1.29 (18H, m). ESI-MS: *m/z* 1011.3 [M+H]<sup>+</sup>.

### Synthesis of NPR1

**4** (30 mg, 0.030 mmol) and Lawesson's reagent (12 mg, 0.030 mmol) were suspended in benzene (5 mL) and refluxed for 3 h. CH<sub>2</sub>Cl<sub>2</sub> (10 mL) was added and the reaction mixture was washed with water (2x 10 mL). The organic portion was then dried over Na<sub>2</sub>SO<sub>4</sub>. The solvent was removed and the crude residue was purified by column chromatography (1:2 v/v EtOAc:hexane) to give the product as yellow solid. Yield: 20 mg (64.9%, R<sub>f</sub> = 0.70). <sup>1</sup>H NMR (500 MHz, CDCl<sub>3</sub>): δ 8.59 (1H, d), 8.51 (1H, d), 8.44 (1H, d), 7.90 (1H, d), 7.70 (1H, t), 7.58-7.60 (3H, m), 7.25-7.27 (2H, m), 7.20 (1H, d), 6.85 (2H, m), 6.35 (4H, m), 4.48 (2H, t), 4.05 (2H, q), 3.74 (4H, m), 3.25-3.36 (12H, m), 1.90 (4H, m), 1.74 (2H, m), 1.20-1.29 (18H, m). <sup>13</sup>C NMR (75 MHz, CDCl<sub>3</sub>): δ 12.27, 13.22, 25.01, 26.89, 30.37, 36.89, 45.21, 47.45, 50.29, 55.22, 73.67, 90.26, 115.47, 116.33, 121.96, 123.77, 126.11, 126.41, 127.05, 129.61, 130.85, 131.29, 131.83, 132.18, 133.10, 133.86, 134.35, 136.45, 152.29, 158.43, 164.75, 165.28, 196.03. ESI-MS: *m/z* 1027.2 [M+H]<sup>+</sup>. Anal. Calcd. for C<sub>60</sub>H<sub>62</sub>N<sub>6</sub>O<sub>4</sub>S<sub>3</sub>: C 70.15, H 6.08, N 8.18. Found: C 70.31, H 6.42, N 8.37.

### Fluorescence studies

**NPR1** was dissolved in DMSO to obtain 1 mM stock solution. K<sub>2</sub>PtCl<sub>4</sub> and Pt<sup>II</sup> complexes were prepared as 1 mM stock solutions in H<sub>2</sub>O. Pt<sup>IV</sup> complexes were prepared as 1 mM stock solutions in DMSO. Fluorescence experiments were carried out by incubating **NPR1** dissolved in CH<sub>3</sub>CN/HEPES buffer (v/v=7:3, 5 mM, pH 7.4) with various amounts of Pt<sup>2+</sup> or Pt complexes at 25 °C and 37 °C respectively for 4 h. The detection limit for cisplatin was calculated based on fluorescence titration experiment. Fluorescence spectrum of the dyad was measured 10 times to obtain standard deviations (σ) of the blank measurements and the slope was obtained from the plot of intensity ratio against the concentrations of cisplatin. Job's plot was carried out with a total [**NPR1**] and [Pt<sup>2+</sup>] concentration of 50 μM by varying the mole fraction of Pt<sup>2+</sup> from 0 to 1. NaCl, KCl, MgCl<sub>2</sub>, NiCl<sub>2</sub>, CuSO<sub>4</sub>, ZnCl<sub>2</sub>, FeSO<sub>4</sub> and FeCl<sub>3</sub> were used as the source of metal ions. Selectivity of the dyad towards various metal ions was carried out by incubating the dyad with metal ions at 25 °C. Competitive assays were carried out by incubating the dyad together with cisplatin and other metal ions at 37 °C. pH response studies of the dyad was measured from pH 3–11.6 by substituting buffers of different pH while keeping the final buffer concentrations constant. pH 3–6 were measured using 200 mM AcOH/AcO<sup>-</sup> buffer, pH 7.4 was measured using 50 mM HEPES buffer and pH 8.4–11.6 were measured with 100 mM H<sup>+</sup>/HPO<sub>4</sub><sup>-</sup> buffer.

### Ratiometric fluorescence imaging of Pt-based drugs

HeLa cells were cultured in Dulbecco's modified Eagle's medium (DMEM) supplemented with 10 % FBS and 1 % antibiotics at 37 °C with 5 % CO<sub>2</sub>. Cells were seeded on cover slips in 6-well plates at a density of 20 x 10<sup>4</sup> cells per mL and incubated overnight. The cells were washed with PBS buffer twice and incubated with Pt<sup>II</sup> or Pt<sup>IV</sup> complexes (30 μM) for 3 h at 37 °C. Subsequently, the cells were washed with PBS buffer thrice, fixed with 4% paraformaldehyde for 15 min and then washed thrice with PBS buffer. The treated cells were then incubated with **NPR1** (20 μM) for 4 h at 37 °C and washed thrice with PBS buffer. The control experiments were prepared by incubating the fixed cells with probe only at 37 °C for 4 h and washed with PBS buffer thrice. The cover slips were mounted onto glass slides in a mounting medium and fluorescence images were acquired with Olympus FluoView FV1000 (Olympus, Japan) laser scanning confocal microscope, with 488 nm laser as the excitation source.

## Acknowledgements

The authors gratefully acknowledge financial support from Ministry of Education and the National University of Singapore (R143-000-A66-112).

## Conflict of Interest

The authors declare no conflict of interest.

**Keywords:** Platinum Drugs • Cisplatin • Fluorescent Probes • Ratiometric • Through Bond Energy Transfer

- [1] a) D. Wang, S. J. Lippard, *Nat. Rev. Drug Discov.* **2005**, *4*, 307-320; b) L. Kelland, *Nat. Rev. Cancer* **2007**, *7*, 573-584.
- [2] a) M. A. Fuertes, C. Alonso, J. M. Pérez, *Chem. Rev.* **2003**, *103*, 645-662; b) M. A. Fuertes, J. Castilla, C. Alonso, J. M. Perez, *Curr. Med. Chem. - Anti-Cancer Agents* **2002**, *2*, 539-551.
- [3] a) M. D. Hall, T. W. Hambley, *Coord. Chem. Rev.* **2002**, *232*, 49-67; b) M. D. Hall, H. R. Mellor, R. Callaghan, T. W. Hambley, *J. Med. Chem.* **2007**, *50*, 3403-3411.
- [4] a) W. H. Ang, S. Pilet, R. Scopelliti, F. Bussy, L. Juillerat-Jeanneret, P. J. Dyson, *J. Med. Chem.* **2005**, *48*, 8060-8069; b) C. F. Chin, Q. Tian, M. I. Setyawati, W. Fang, E. S. Tan, D. T. Leong, W. H. Ang, *J. Med. Chem.* **2012**, *55*, 7571-7582; c) S. Q. Yap, C. F. Chin, A. H. H. Thng, Y. Y. Pang, H. K. Ho, W. H. Ang, *ChemMedChem* **2017**, *12*, 300-311.
- [5] a) D. Y. Q. Wong, J. Y. Lau, W. H. Ang, *Dalton Trans.* **2012**, *41*, 6104-6111; b) D. Y. Q. Wong, J. H. Lim, W. H. Ang, *Chem. Sci.* **2015**, *6*, 3051-3056.
- [6] a) W. H. Ang, I. Khalaila, C. S. Allardyce, L. Juillerat-Jeanneret, P. J. Dyson, *J. Am. Chem. Soc.* **2005**, *127*, 1382-1383; b) S. Dhar, S. J. Lippard, *Proc. Natl. Acad. Sci. U.S.A.* **2009**, *106*, 22199-22204; c) L. Ma, R. Ma, Y. Wang, X. Zhu, J. Zhang, H. C. Chan, X. Chen, W. Zhang, S. K. Chiu, G. Zhu, *Chem. Commun.* **2015**, *51*, 6301-6304.
- [7] a) A. E. Egger, C. Rappel, M. A. Jakupec, C. G. Hartinger, P. Heffeter, B. K. Keppler, *J. Anal. At. Spectrom.* **2009**, *24*, 51-61; b) S. I. Kirin, I. Ott, R. Gust, W. Mier, T. Weyhermüller, N. Metzler-Nolte, *Angew. Chem. Int. Ed.* **2008**, *47*, 955-959; c) A. Ghezzi, M. Aceto, C. Cassino, E. Gabano, D. Osella, *J. Inorg. Biochem.* **2004**, *98*, 73-78.
- [8] a) C. Molenaar, J.-M. Teuben, R. J. Heetebrij, H. J. Tanke, J. Reedijk, *J. Biol. Inorg. Chem.* **2000**, *5*, 655-665; b) R. Safaei, K. Katano, B. J. Larson, G. Samimi, A. K. Holzer, W. Naerdemann, M. Tomioka, M. Goodman, S. B. Howell, *Clin. Cancer Res.* **2005**, *11*, 756-767; c) X.-J. Liang, D.-W. Shen, K. G. Chen, S. M. Wincovitch, S. H. Garfield, M. M. Gottesman, *J. Cell. Physiol.* **2005**, *202*, 635-641; d) M. A. Miller, B. Askevold, K. S. Yang, R. H. Kohler, R. Weissleder, *ChemMedChem* **2014**, *9*, 1131-1135.
- [9] a) E. J. New, R. Duan, J. Z. Zhang, T. W. Hambley, *Dalton Trans.* **2009**, 3092-3101; b) J. J. Wilson, S. J. Lippard, *Inorg. Chim. Acta.* **2012**, *389*, 77-84; c) Y. Song, K. Suntharalingam, J. S. Yeung, M. Royzen, S. J. Lippard, *Bioconjugate Chem.* **2013**, *24*, 1733-1740; d) Y. Yuan, Y. Chen, B. Z. Tang, B. Liu, *Chem. Commun.* **2014**, *50*, 3868-3870.
- [10] a) S. Wu, X. Wang, C. Zhu, Y. Song, J. Wang, Y. Li, Z. Guo, *Dalton Trans.* **2011**, *40*, 10376-10382; b) S. Wu, C. Zhu, C. Zhang, Z. Yu, W. He, Y. He, Y. Li, J. Wang, Z. Guo, *Inorg. Chem.* **2011**, *50*, 11847-11849.
- [11] a) C. Shen, B. D. Harris, L. J. Dawson, K. A. Charles, T. W. Hambley, E. J. New, *Chem. Commun.* **2015**, *51*, 6312-6314; b) J. L. Kolanowski, L. J. Dawson, L. Mitchell, Z. Lim, M. E. Graziotto, W. K. Filipek, T. W. Hambley, E. J. New, *Sens. Actuators B Chem.* **2018**, *255*, 2721-2724.
- [12] a) D. Montagner, S. Q. Yap, W. H. Ang, *Angew. Chem. Int. Ed.* **2013**, *52*, 11785-11789; b) J. X. Ong, J. Y. Yap, S. Q. Yap, W. H. Ang, *J. Inorg. Biochem.* **2015**, *153*, 272-278; c) J. X. Ong, C. S. Q. Lim, H. V. Le, W. H. Ang, *Angew. Chem. Int. Ed.* **2019**, *58*, 164-167.
- [13] a) G.-S. Jiao, L. H. Thoresen, K. Burgess, *J. Am. Chem. Soc.* **2003**, *125*, 14668-14669; b) R. Bandichhor, A. D. Petrescu, A. Vespa, A. B. Kier, F. Schroeder, K. Burgess, *J. Am. Chem. Soc.* **2006**, *128*, 10688-10689; c) W. Lin, L. Yuan, Z. Cao, Y. Feng, J. Song, *Angew. Chem. Int. Ed.* **2010**, *49*, 375-379.
- [14] a) H. Yu, Y. Xiao, H. Guo, X. Qian, *Chem. Eur. J.* **2011**, *17*, 3179-3191; b) J. Fan, P. Zhan, M. Hu, W. Sun, J. Tang, J. Wang, S. Sun, F. Song, X. Peng, *Org. Lett.* **2013**, *15*, 492-495; c) H. Yu, L. Jin, Y. Dai, H. Li, Y. Xiao, *New J. Chem.* **2013**, *37*, 1688-1691; d) L. Zhou, X. Zhang, Q. Wang, Y. Lv, G. Mao, A. Luo, Y. Wu, Y. Wu, J. Zhang, W. Tan, *J. Am. Chem. Soc.* **2014**, *136*, 9838-9841; e) L. Zhou, Q. Wang, X. B. Zhang, W. Tan, *Anal. Chem.* **2015**, *87*, 4503-4507; f) J. X. Ong, V. Y. T. Pang, L. M. Tng, W. H. Ang, *Chem. Eur. J.* **2018**, *24*, 1870-1876.
- [15] B. Zhu, C. Gao, Y. Zhao, C. Liu, Y. Li, Q. Wei, Z. Ma, B. Du, X. Zhang, *Chem. Commun.* **2011**, *47*, 8656-8658.
- [16] H. Yu, Y. Xiao, H. Guo, *Org. Lett.* **2012**, *14*, 2014-2017.
- [17] S. C. Dhara, *Indian J. Chem.* **1970**, *8*, 193-194.
- [18] M. Galanski, S. Slaby, M. A. Jakupec, B. K. Keppler, *J. Med. Chem.* **2003**, *46*, 4946-4951.
- [19] A. R. Battle, R. Choi, D. E. Hibbs, T. W. Hambley, *Inorg. Chem.* **2006**, *45*, 6317-6322.
- [20] K. S. Lovejoy, R. C. Todd, S. Zhang, M. S. McCormick, J. A. D'Aquino, J. T. Reardon, A. Sancar, K. M. Giacomini, S. J. Lippard, *Proc. Natl. Acad. Sci. U.S.A.* **2008**, *105*, 8902-8907.

